



UNITED
TECHNOLOGIES
RESEARCH
CENTER

East Hartford
Connecticut 06108

12

DTIC FILE COPY

AD-A187 368

September 14, 1987

Department of the Navy
Code 431
800 N. Quincy Street
Arlington, VA 22216

Attention: Dr. Ralph Judy

Gentlemen:

The Annual Report is hereby submitted in accordance with
the requirements of contract number N00014-85-C-0421.

Sincerely yours,

UNITED TECHNOLOGIES CORPORATION
Research Center

N. S. Bornstein
Chief Materials Process Research

encl.

DTIC
ELECTE
OCT 20 1987
S D

DISTRIBUTION STATEMENT A

Approved for public release
Distribution Unlimited

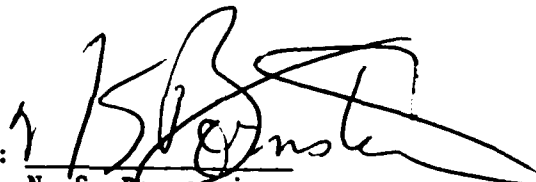
Study of Adherent Oxide Scales
Contract No. N00014-85-C-0421

R87-917259-1

Reported by:

J. G. Smeggil
N. S. Bornstein

Approved by:


N. S. Bornstein
Program Manager



| | |
|----------------------------------|--|
| 1. Name of Contractor | |
| 2. Name of Project | |
| 3. Name of Inspector | |
| 4. Date of Inspection | |
| 5. Location of Inspection | |
| 6. Description of Inspection | |
| 7. Results of Inspection | |
| 8. Remarks | |
| 9. Signature of Inspector | |
| 10. Signature of Project Manager | |

per ltr

A-1

Unclassified

SECURITY CLASSIFICATION OF THIS PAGE

N00014-85-C-0421

REPORT DOCUMENTATION PAGE

| | | | | |
|---|-------|--|---|--------------------|
| 1a. REPORT SECURITY CLASSIFICATION Unclassified | | | 1b. RESTRICTIVE MARKINGS | |
| 2a. SECURITY CLASSIFICATION AUTHORITY | | | 3. DISTRIBUTION / AVAILABILITY OF REPORT | |
| 2b. DECLASSIFICATION / DOWNGRADING SCHEDULE | | | | |
| 4. PERFORMING ORGANIZATION REPORT NUMBER(S) | | | 5. MONITORING ORGANIZATION REPORT NUMBER(S) | |
| 6a. NAME OF PERFORMING ORGANIZATION United Technologies Research Center | | 6b. OFFICE SYMBOL (if applicable) | 7a. NAME OF MONITORING ORGANIZATION | |
| 6c. ADDRESS (City, State, and ZIP Code) Silver Lane East Hartford, CT 06108 | | | 7b. ADDRESS (City, State, and ZIP Code) | |
| 8a. NAME OF FUNDING / SPONSORING ORGANIZATION Office of Naval Research | | 8b. OFFICE SYMBOL (if applicable) | 9. PROCUREMENT INSTRUMENT IDENTIFICATION NUMBER | |
| 8c. ADDRESS (City, State, and ZIP Code) Department of the Navy Arlington, VA 22217 | | | 10. SOURCE OF FUNDING NUMBERS | |
| | | | PROGRAM ELEMENT NO. | PROJECT NO. |
| 11. TITLE (Include Security Classification) Study of Adherent Oxide Scales | | | | |
| 12. PERSONAL AUTHOR(S) J. G. Smeggil, N. S. Bornstein | | | | |
| 13a. TYPE OF REPORT Annual Technical | | 13b. TIME COVERED FROM 2/28/86 TO 4/30/87 | 14. DATE OF REPORT (Year, Month, Day) | 15. PAGE COUNT |
| 16. SUPPLEMENTARY NOTATION | | | | |
| 17. COSATI CODES | | | 18. SUBJECT TERMS (Continue on reverse if necessary and identify by block number) Oxidation, Oxide Scale Adherence, Oxide Scale Formation, Minor Element Effects, Sulfur | |
| FIELD | GROUP | SUB-GROUP | | |
| | | | | |
| | | | | |
| 19. ABSTRACT (Continue on reverse if necessary and identify by block number) The bond between alumina and NiCrAl substrate is intrinsically strong. The segregation of sulfur to the interface reduces bond strength, sulfur is present at the interface in both compound and apparently elemental form as determined from ESCA studies. | | | | |
| 20. DISTRIBUTION / AVAILABILITY OF ABSTRACT <input type="checkbox"/> UNCLASSIFIED/UNLIMITED <input type="checkbox"/> SAME AS RPT. <input type="checkbox"/> DTIC USERS | | | 21. ABSTRACT SECURITY CLASSIFICATION | |
| 22a. NAME OF RESPONSIBLE INDIVIDUAL | | | 22b. TELEPHONE (Include Area Code) | 22c. OFFICE SYMBOL |

I. INTRODUCTION

All structural alloys are, with respect to oxygen, thermodynamically unstable and react to form scales. For many alloys, a protective scale limits the accessibility of oxygen to the substrate thereby increasing the useful life of the material. However, in general the useful life is controlled not by the passage of diffusing species through growing oxide scales but by the frequency of scale spallation.

Improved oxide scale adherence through the addition of low levels of reactive elements such as yttrium has been repeatedly documented in the literature. Despite extensive research in this area, agreement on a single mechanism to account for scale adherence benefits is lacking. The identification of the factors responsible for oxide scale adherence has been the subject of intensive investigations for several decades, and numerous mechanisms have been proposed to account for the factors thought to be important for oxide scale adherence. These include:

- (a) The formation of pegs which "anchor" the scale to the substrate (1).
- (b) The prevention of vacancy coalescence at scale substrate interface by providing alternative sites (2).
- (c) Increased scale plasticity (3).
- (d) Modification of scale growth process (4).
- (e) Formation of graded scale minimizing thermo-mechanical differences (5) and,
- (f) Modification of bonding forces through preferential segregation (6).

At UTRC it was shown that laser melting and rapid solidification of thin surface layers on MCrAlY coatings further improved oxide adherence over and above that observed for yttrium additions.

For example, shown in Fig. 1 are photo-micrographs of the surfaces after 100 hours of testing of a MCrAlY coated nickel base superalloy. One surface was exposed to a 7 Kw laser beam prior to testing. The oxide scale which then formed on this surface during test is so thin that the "laser passes" are still visible through the film. The oxide scale formed on the reverse side exhibits the molted scale typical of a surface which has formed, spalled and reformed an oxide many times. Thus, the initial objective of the program was the characterization of effect (a) by which laser-processing and minor element additions improve oxide scale adherence of a NiCrAl turbine coating composition. However, it was shown at the completion of the first year that sulfur, an indigenous impurity in the material, caused the oxide scale to spall. Thus the objective of the study changed to defining the role of sulfur with respect to oxide scale adherence and elucidate the role of the reactive elements with respect to oxide scale adherence. However, significant observations were made with respect to the morphology of the oxide scale that forms on NiCrAl and NiCrAlY and these are summarized as follows:

1. A uniformly thick, poorly adherent scale formed on NiCrAl. It is composed chiefly of large columnar grains. The surface structure of the oxide suggested porosity the depth of which could not be established from surface examinations. The metal below the oxide scale exhibited features which are construed to be Kirkendall voids. However the density of voids are few and are not believed to be responsible for the extensive degree of scale spallation. Figure 2 is photomicrograph of the oxide scale which forms on NiCrAl and a schematic showing the characteristics of the scale is presented in Fig. 3a.

2. An adherent multilayer scale formed on the surface of NiCrAlY exposed 24 hours at 1050°C. A diamond scribe was used to abrade the oxidized surface in order to characterize the scale in cross-section without the complications associated with polishing and etching. Over the gamma phase, a three-zone oxide layer was observed, Fig. 3b. The outermost layer which appeared flat was about 0.1 micrometers thick. Below this layer a fine grained porous appearing zone was observed. Immediately adjacent to this and extending to the metal substrate below was a relatively large grained apparently columnar oxide, approximately 1.5 micrometer thick. Lastly, a sparse number of voids were noted. It could not be determined if the voids were Kirkendall effects or the result of micropegs pulled when the scale locally exfoliated.

3. A two zone oxide formed over the beta phase, Fig. 4. An outer layer of nodular oxide growth which visually appeared porous had grown to a thickness of about 2.8 micrometers. Below this layer, a zone of large grained columnar oxide, about 1.5 micrometers thick had developed. It is noted that the thickness of the columnar grained layer in contact with the metal was the same regardless of whether it was formed over the gamma or the beta phase.

4. Diamond scribing was also used to examine the oxide scale that formed on the laser processed NiCrAlY specimens. The oxide structure consists of two layers, Fig. 3c. The outermost layer formed a large number of alumina whisker-like growths on the surface. This layer was about 2.5 microns thick and porous, Fig. 5. The inner most layer was approximately 0.5 microns thick and was essentially comprised of small equiaxed grains. In contrast, the oxidized "as annealed" NiCrAlY similarly tested showed a thick zone about 1.5 microns thick, of columnar grains adjacent to the metal. Lastly, although the interface between the oxide scale and the substrate metal was characterized by considerable microporosity, the scale was strongly adherent.

Experimental Procedure

Alloys were prepared based upon Ni-20 wt pct Cr-12 wt. pct Al (NiCrAl) with minor element additions by vacuum melting 2 cm diameter rods in alumina crucibles. The nickel and aluminum used were 99.9 pct pure and the chromium was 99.99 pct pure. The cast alloys were homogenized at 1200°C for 48 hours. Minor element additions included yttrium, yttrium sulfide (Y_2S_3) and iron sulfide, (FeS).

Cyclic oxidation tests were conducted at 1050 and 1180°C (55 min hot - 5 min cool) for up to 1000 hours. Mass decrease indicates scale exfoliation which is always visually confirmed.

Initial Auger studies were conducted using a model 540 scanning microprobe. Figure 6, shows the configuration of the specimen, sample heater, electron gun, cylindrical mirror analyzer and ion sputter gun. The heater consisted of a resistance heated niobium wire filament surrounded by tantalum heat shields to which the specimen was clamped facing the electron beam and analyzer. A Varian Analog System Model VI-18 was later modified and differed primarily with the substitution of platinum wire as opposed to niobium wire for the heating of the specimens. Lastly, a Perkin Elmer PHI-610 Auger/ESCA spectrometer was also used in this study and special techniques were developed to examine oxide scales. It should be noted that the oxide scale formed at 600°C is quite tenacious and does not readily spall. However, the oxide scale that forms after exposure for 45 min at 1050°C is virtually completely exfoliated and therefore cannot be brought intact into the Auger/ESCA environment. However, through a process of trial and error, it was experimentally determined that the oxide scale formed when NiCrAl is exposed at 1050°C for 20-25 min. appears adherent but when viewed with the scanning electron microscope contains cracks and fissures within the scale. Various glues were examined and determined to be free of sulfur. An aluminum block was attached to the oxide scale through the organic glue which allowed removal of the scale within the Auger chamber.

The following sequence of Auger procedures was used: (a) evacuation of the chamber to 10^{-9} torr, (b) chamber back fill with argon and ion sputter etching (2 Kv, 30 Ma) to remove atmospheric surface contamination, (c) chamber evacuation to 10^{-9} torr, (d) specimen heating and Auger analysis, (e) chamber backfill with argon and ion sputter etching and Auger analysis to provide chemical depth profiling. Estimated surface compositions were obtained from Auger spectra by measuring peak heights and using elemental sensitivity factors as discussed in the "Handbook of Auger Spectroscopy" (7). Lastly, it should be noted that a thermocouple spot welded to the sample was used to monitor temperature. Samples were heated to temperature between 700 and 1000°C. Surface composition was monitored as a function of time at each temperature until steady state conditions were obtained. Several Auger spectra were then recorded.

Experimental Results

1. Auger Studies

Typical auger spectra for NiCrAl at room temperature, 700°C and 1000°C are shown in Fig. 7. With increasing temperature the dominant surface species is sulfur. The calculated surface concentration of sulfur for NiCrAl and NiCrAlY alloys (with and without preheat sputter cleaning) are shown as a function of temperature in Fig. 8. Note that the sulfur concentrations were much higher on the NiCrAl (approximately 20 at. pct) than on NiCrAlY (approximately 5 at. pct) and increased very slightly with temperature. Subsequent chemical depth profiling using argon ion sputtering showed that sulfur was present in a layer less than 20A thick.

Attached to the Perkin Elmer PHI 610 unit is a residual gas analyzer. At 600°C both SO and SO₂ are observed. For a total system pressure of 8×10^{-8} torr, the maximum SO₂ height corresponds to about 10^{-11} torr or 0.125% of the total residual gas. In comparison the water pressure corresponds to 10×10^{-10} torr. Moreover, the sulfur-bearing gases are not detected unless the MCrAl(Y) specimens are present and heated.

Scanning auger electron micrographs were taken to characterize the distribution of elements present on the surfaces of the NiCrAl specimens. Oxygen is present on the surfaces of both the gamma and beta phases. Surface oxygen enrichments form because of the reaction of the heated metal surface with the H₂O present in the residual gases. Of significance is the observation that surface sulfur segregation occurs principally on the gamma phase which is rich in chromium.

2. Oxidation Studies

The cyclic oxidation tests were conducted at 1050 and 1180°C (55 minutes at temperature, and 5 minutes at room temperature) and are presented in terms of mass change per unit area as a function of time. A negative mass change indicates scale exfoliation.

There is little doubt that the presence of very small amounts of elemental yttrium significantly improve the ability of the NiCrAl alloy to resist scale spallation, as shown in Fig. 9.

An increase in the nominal sulfur content of the NiCrAl alloy from about 50 ppm to 300 ppm (by the addition of FeS) did not significantly change the cyclic oxidation behavior of the alloy (Fig. 9). However, when the same amount of sulfur was added to the NiCrAlY composition, the alloy did not form an adherent oxide scale, and the oxidation behavior of the sulfur doped NiCrAlY alloy was for all practical purposes identical to that of the NiCrAl alloy. Lastly, when additional yttrium was added to the sulfur doped (FeS) NiCrAlY alloy, the ability of the alloy to form an adherent oxide scale was restored. However, although the data strongly suggests that sulfur is the principle agent effecting the adherence of the oxide scale, both sulfur and iron were introduced into the alloy.

Yttrium sesquisulfide is a stable compound and in a series of experiments was used along with elemental yttrium in order to further illustrate their individual roles with respect to oxide scale adherence. The addition of elemental yttrium prevented oxide scale exfoliation as once again demonstrated by the small mass increase, (NiCrAlY vs NiCrAl, Fig.10). With yttrium sulfide (Y₂S₃) additions, severe scale exfoliation ensued resulting in large mass losses. Lastly, when both elemental yttrium and yttrium sulfide were added, good oxide scale adherence and slight mass increases were effected.

Similar results were observed when the same tests were performed at 1180°C. The baseline alloy NiCrAl showed mass losses almost from the inception of the test, Fig. 11. With the addition of elemental yttrium to the baseline composition, oxide scale adherence was enhanced. However, when yttrium was added to the baseline alloy as the sesquisulfide (Y_2S_3), oxidation resistance was severely degraded, Fig. 11. Only with the addition of elemental yttrium to the Y_2S_3 -containing alloys, were good oxide scale and protective kinetics re-engendered.

3. Microscopy Studies

The overall phase distribution of the NiCrAl alloys has been well documented (8,9) and the principal metallic phases were the gamma nickel solid solution and the intermetallic phase NiAl. At room temperature, alpha chromium precipitates were visible within the NiAl matrix. In addition to the metallic phases, fine inclusions were observed and these were identified based upon electron microbeam studies to be enriched in aluminum and oxygen.

In addition to the oxide inclusions, precipitates were observed which were enriched in sulfur. Indeed, numerous sulfur containing particles were found randomly dispersed along with oxide particles within the NiCrAl alloy (10). It was also reported that the sulfur-containing particles were enriched in aluminum and/or chromium.

The addition of yttrium to the NiCrAl alloy resulted in the precipitation of nickel yttride phases. It was also noted that for specimens examined several days after polishing that the nickel yttride phase particles were essentially converted to a yttrium-enriched oxide phase. This room temperature oxidation has been previously reported (11). Lastly, of note was the absence of numerous sulfur rich particles in the NiCrAlY alloy. After extensive examination of several specimens, only a singular particle enriched in sulfur was noted in the NiCrAlY. The sulfur enriched particle also contained both yttrium and oxygen.

Extensive microscopy studies were performed on NiCrAl and NiCrAlY specimens oxidized for up to 100 hours at temperatures to 1180°C. Although the oxide scale that forms on NiCrAl spalls, areas exhibiting partially adherent scales were identified, metallographically mounted and polished. In examination by the electron microbeam probe in line scan mode, regions of the specimens with alumina scales still adherent showed sulfur enrichments at the scale-metal interface, Fig. 12. The same technique was used to examine the scale-metal interfaces for NiCrAlY specimens; however, no similar sulfur enrichments were found.

To discern more closely if sulfur enrichments were to be found at the scale-metal interface of oxidized NiCrAlY specimens, the surfaces were examined by scanning transmission electron microscopy. The scales were mechanically removed, and particles present at the scale-metal interface were examined. In the case of both isothermally and cyclically tested specimens, numerous sub-micron particles were detected. However, whenever a particle was identified as having an yttrium-enrichment concomitantly a sulfur-enrichment was also observed.

4. ESCA Studies

Electron Spectroscopy for Chemical Analysis (ESCA) also known as X-ray Photoelectron Spectroscopy (XPS) is an analytical technique for investigating the chemical composition of solid surfaces. It involves irradiation of the solid in vacuo with monoenergetic soft x-rays. Quantitative data is obtained from peak heights and identification of chemical states is made from the position and separations of peaks and spectral contours.

The binding energy for sulfur and its compounds is shown in Fig. 13. There is limited data for metallic sulfides and therefore, a portion of this study is devoted to the generation of specific data for the sulfide or nickel, chromium, and aluminum.

Ions of sulfur were implanted in Ni, Cr, Al, NiCrAl, NiCrAlY and Al_2O_3 . A Varian/Extrion Model 200 CFS ion implanter was used in this study. The specimens were mechanically clamped to a liquid cooled substrate holder. A typical implant schedule is shown below.

| <u>Energy Level</u> | <u>Dose</u> |
|---------------------|----------------------|
| keV | ions/cm ² |
| 200 | 2×10^{17} |
| 80 | 5.4×10^{16} |
| 30 | 2.5×10^{16} |

Figure 14 is typical of the data generated for sulfur doped aluminum. In general, it is possible to identify the outer oxide scale, an inner zone richer in sulfur and the matrix alloy. From these studies the Research Center experimentally determined the binding energy for the metal sulfides of interest and these values are listed in Fig. 15. It is concluded that for all practical purposes, the similarity in binding energies of the sulfides preclude individual identification. However, it is possible to separate sulfide from elemental sulfur.

ESCA survey studies of sputter cleaned specimens at room temperature and at 600°C clearly indicated peaks associated with the major components present, i.e. Ni, Cr, Al and O. Nothing unusual was observed in their peak position.

Relevant to the studies conducted here, ESCA data collected for surface segregated sulfur for relatively short times, i.e. approximately 2 min. with the specimen at 600°C, yielded a very noisy binding energy curve, Fig. 16. The only point that could be made for this short time data was that a peak was likely present at 162 ev. That peak could be associated with S^{-2} (8).

However long term collection of ESCA data for the surface segregated sulfur was also performed. After nine hours of data collection, an unsymmetrical peak was observed for the surface segregated sulfur, Fig. 17. With the assistance of ESCA data taken on an elemental sulfur specimens, it was possible to deconvolute the asymmetric peak to two peaks: one at 164 ev and one at 162 ev, Fig. 18.

Based on both literature data for inorganic sulfides and ESCA measurements on chromium sulfide, nickel sulfide and aluminum sulfide, the peak at 162 ev was associated with the S^{2-} moiety. With the resolution of the ESCA used in studies conducted here, it was not possible to determine whether this was a nickel-, chromium-, aluminum-sulfide or some mixture of any of all of the sulfides of these metals.

The peak at 164 ev on the NiCrAl specimen matched the peak for elemental sulfur. A curve fitting program determined that the total area peak associated with all sulfur-bearing species in Fig. 18, is comprised of a 20% contribution from the elemental sulfur and an 80% contribution from S^{2-} .

DISCUSSION

It is well documented that low levels of reactive elements such as yttrium markedly improve oxide scale adherence. The mechanisms proposed to account for the improvements have been previously described. The lack of agreement on a single mechanism, despite extensive research, may indicate that the actual mechanism has yet to be identified.

A new mechanism is herein proposed. It is proposed that the bond between the normally protective alumina scale and the substrate alloy is quite strong. However, sulfur present within the alloy segregates to and weakens the bond thereby promoting scale exfoliation. It is further proposed that reactive element additions reduce sulfur segregation to the oxide scale-metal interface, thereby improving scale adherence. Because the reactive elements which improve scale adherence (yttrium, hafnium, etc.) are strong sulfide formers, they can reduce sulfur segregation by: (1) reacting with sulfur during liquid phase processing thereby removing sulfur from the alloy; or (2) reacting with sulfur in the solid state, thereby producing a refractory sulfide and lessening the concentration of sulfur in solution which is able to segregate. When the reactive elements are added as oxides, their role may be to additionally provide an increased amount of oxide-metal interface, thereby reducing the amount of sulfur available for segregation to the critical protective oxide-metal interface. This is in addition to the reaction of the oxides to form stable oxysulfides.

In support of the proposed mechanism, the strength of grain boundaries in nickel alloys can be improved by an analogous mechanism. In the absence of reactive elements, sulfur segregates to and embrittles grain boundaries, (12-15). Additions of reactive elements have been shown to reduce sulfur segregation and improve grain boundary strength (14, 15).

A close relationship exists between the elements which segregate to grain boundaries and those which segregate to exterior surfaces although differences are noted in enrichment ratios and other segregation characteristics (16). Both surface and grain boundary segregation are derived by reduced interfacial energy and by the energy reduction achieved when a solute atom which fits poorly in a matrix lattice (due to size or electronic considerations) moves to the more open interfacial structure. Sulfur has been repeatedly observed to segregate to the exterior surfaces of nickel and nickel base superalloys (17-23).

NiCrAl and NiCrAlY both form alumina scales when they are exposed in air at elevated temperatures. However, the scales that form on the surface of the NiCrAl alloy spall. The addition of sulfur in the form of iron sulfide does not improve oxide scale adherence with respect to the NiCrAl specimens. Most important however, the addition of the sulfur does cause the scale that forms on the NiCrAlY alloy to spall. The ability of the alloy to form an adherent spall resistant oxide scale is re-established only when additional quantities of yttrium are added to the alloy. Thus, these results strongly imply that a relationship exists between sulfur, yttrium and iron and the ability of the alloy to resist oxide scale spallation.

In order to eliminate the role of iron and establish the relationship between sulfur, yttrium and oxide scale spallation, yttrium was added as the element and as the sesquisulfide. Sulfur was added only as the sesquisulfide.

As previously noted, it is well established that minor additions of elemental yttrium or the oxide markedly improves oxide scale adherence. However as is clearly shown in this study the addition of yttrium as the sesquisulfide did not impart beneficial oxide scale adherence effects. The addition of Y_2S_3 to NiCrAl actually increased the rate at which the alloy lost mass. This result clearly establishes the fact that the addition of a source of yttrium is in itself insufficient to improve resistance to scale exfoliation.

The addition of yttrium to NiCrAl imparts resistance to scale exfoliation. The addition of yttrium to the NiCrAl + Y_2S_3 alloy also imparts resistance to scale exfoliation. Yttrium imparts resistance to scale spallation to alloys which contain sulfur. With respect to the latter, the yttrium sesquisulfide is the source of "free" sulfur for the alloy. Although the phase diagram for the yttrium-sulfur system has not been reported, the most metal-rich-yttrium-sulfur phase reported is the monosulfide, YS. If in the alloy the sesquisulfide phase were to decompose to the monosulfide, then additional "free" sulfur would be liberated:



Even if the yttrium sesquisulfide did not decompose to the most metal-rich yttrium sulfide reported, namely YS, but halted at some intermediate sulfide composition, some sulfur would effectively be added to the alloy. This additional liberated sulfur present within the alloy would exacerbate the oxide scale adherence properties of the alloy. Thus, the role of the additional yttrium is to react with and tie up the excess sulfur.

As previously discussed, sulfur segregates to the free surface. While measurements at 800-1000°C resulted in a calculated surface sulfur concentration of approximately 20 atom percent, at the lower temperature (600°C) an enrichment of only 1.9 atomic percent was noted. However, because the residual gas analyzer revealed both SO and SO₂ in the ambient atmosphere when the Ni-20Cr-12Al specimens were heated, the 1.9% enrichment is not to be construed as a thermodynamic equilibrium as opposed to a steady state value.

The short time ESCA measurements gave evidence for only S⁻² based upon literature data for inorganic sulfides (24) and actual measurements on aluminum-, chromium- and nickel-sulfides. The ESCA data could not be resolved sufficiently to indicate which metal species (or specie) was associated with the S⁻² peak. However, based upon the auger electron maps, the sulfur was associated with chromium enrichments to be found in the gamma phase (25).

Based upon these findings, it could be suggested that at least one role chromium plays in these alloys is to chemically interact with and reduce the thermodynamic activity of the sulfur in the alloy. In support of this suggestion, the reported activity of aluminum₄ in a NiCrAl composition close to that studied here was approximately 6×10^{-4} while that for chromium was approximately 0.5 (26). Given the thermodynamic data for Al₂S₃ and "CrS" (27), calculations indicate that on a per mole S₂ basis "CrS" is more stable than Al₂S₃ in this system at temperatures of 1050 and 1180°C. Specifically using data in (26) for the activities of aluminum and in (27) for the thermodynamic stability of the respective sulfides, the activity of S₂ (9) above chromium and aluminum is calculated to be:

| Temperature °C | Calculated Activity of S ₂ (9) Over | |
|-------------------|--|-----------------------|
| | <u>Aluminum</u> | <u>Chromium</u> |
| 1050 | 1.1×10^{-9} | 1.7×10^{-10} |
| 1180 | 1.9×10^{-7} | 3.8×10^{-9} |

Hence, clearly at least in this temperature range, the chromium in the alloy lowers the sulfur activity greater than that of aluminium.

Despite this ability of chromium to reduce sulfur activities, active elements such as yttrium would reduce it much more. Yttrium sulfide is reported to be far more stable than "CrS" (27,28). Based on available thermodynamic data (28) and assuming an activity for yttrium equal to its mole fraction in the alloy₅₅ the calculated S₂(9) activity over the NiCrAl-0.1Y alloy is 5×10^{-55} and 1.6×10^{-47} at 1050°C and 1180°C, respectively.

The observation of unsymmetrical peaks in the ESCA studies is attributed to the presence of elemental sulfur. These peaks were deconvoluted to one attributable to S_{2s} at 162 ev and one attributable to elemental sulfur at 164 ev. The approximate steady state composition of the overall sulfur peak was 20% elemental sulfur and 80% sulfide.

It should be noted that when viewed with the scanning electron microscope using EDAX techniques, a characteristic sulfur peak would initially appear and then disappear into the background spectrum noise. This observation is consistent with localized regions containing a labile form of sulfur. Elemental sulfur would evaporate under the electron beam and hence explain the labile properties associated with the transient sulfur peaks.

Regarding the order of the sulfur layers, free sulfur could be present (1) as a discrete layer below the sulfide layer, (2) intimately intermingled with the sulfide layer, or (3) as a discrete layer above the sulfide layer adjacent to the oxide scale.

The following model is consistent with all of the aforementioned observation associated with the "rare earth" effect and with the observations made in this study.

With respect to the NiCrAl alloy, initially a thin film of oxide forms on the surface of this two phase alloy. The oxide scale is strongly adherent and resists exfoliation. Glued rods could not separate the freshly formed oxide from the substrate. With time, sulfur segregates to the surfaces and appears to be initially most pronounced to the surface of the gamma phase.

With increased time a sulfide and free sulfur layer are present at the scale-metal interface. This sulfide/sulfur layer then effectively acts as a continuous layer upon which the alumina film grows. Thus, for a yttrium-free NiCrAl alloy, the mature oxide scale appears morphologically uniform regardless whether it has formed over the beta or gamma phases of the alloy.

In the presence of yttrium, sulfur segregation is reduced. In the absence of the sulfide/sulfur layer, the alumina scale that forms on the alloy reflects the nature of the alloy phase (beta or gamma) upon which it is growing. Hence, the more complex oxide morphologies are produced.

SUMMARY AND CONCLUSIONS

. Sulfur is an indigenous impurity present at tramp levels within nickel base alloys. Precipitated sulfides are identified within NiCrAl and NiCrAlY alloys.

Auger studies show that sulfur segregates to free surfaces. Sulfur is identified at the critical oxide scale metal interface.

The addition of sulfur as FeS to NiCrAl+Y causes the alloy to form non-protective oxide scales which readily spall.

The addition of sulfur as Y_2S_3 to NiCrAl+Y causes the normally protective oxide scale to spall.

Sulfur causes the oxide scale to spall. Sulfur is present at the scale-metal interface in compound and elemental form. Based upon the ESCA studies, the approximate steady state composition of the overall sulfur peak is 20 a/o elemental sulfur and 80 a/o sulfide.

In summary, a new and different mechanism is proposed. It is proposed that the alumina scale that forms on NiCrAl alloys are quite adherent. Sulfur in the alloy segregates to and weakens the bonds at the oxide scale-metal interface. The role of the reactive materials which promote oxide scale adherence is to interact with and form stable compounds thereby decrease the migration and concentration of sulfur to the critical oxide scale-metal interface.

LASER SURFACE MELTING IMPROVES OXIDATION RESISTANCE



OXIDE SPALLING



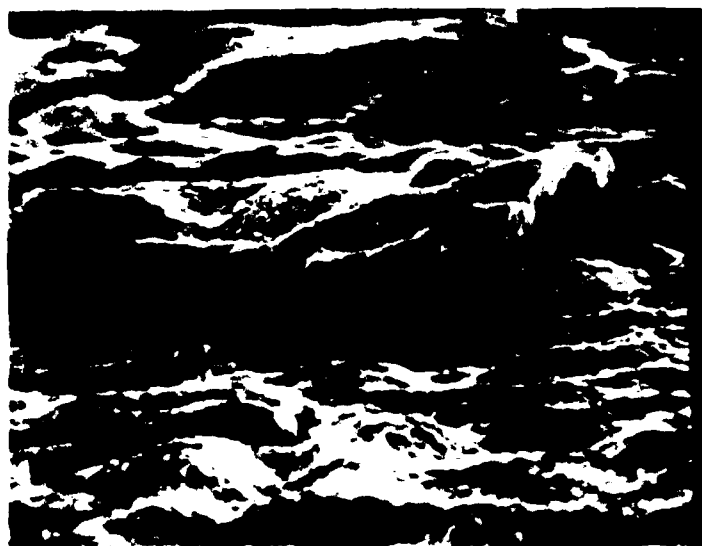
OXIDE ADHERING

1000°C - 100 hrs. CYCLIC BURNER RIG TESTS

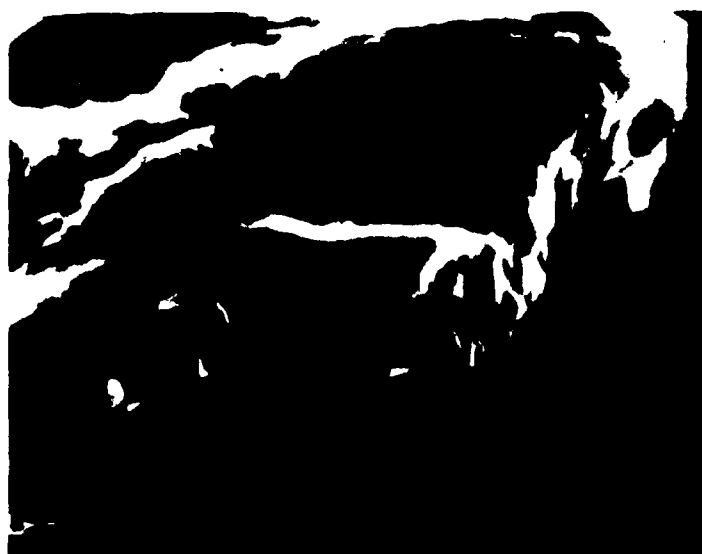
FIG. 1

FIG. 2

COLUMNAR GRAIN STRUCTURE OF OXIDE ON NiCrAl
100 hrs ISOTHERMAL TEST



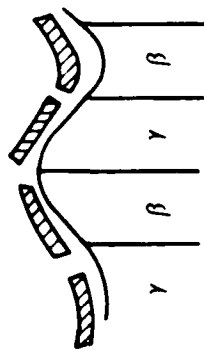
5μm



1μm

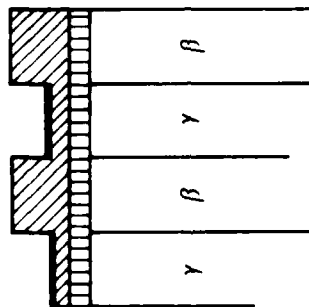
SCHEMATIC REPRESENTATION OF SCALE FORMATION

(a) NiCrAl



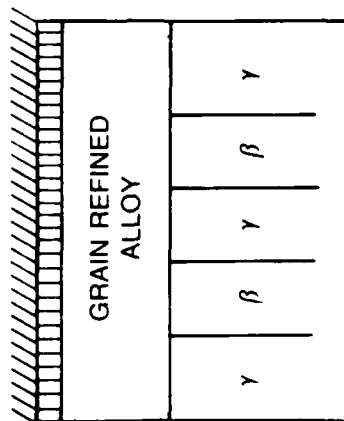
NONADHERENT SCALE
ON UNDULATING
SURFACE

(b) NiCrAlY



ADHERENT OXIDE SCALE:
3 LAYER ON γ , 2 LAYERS
ON β

(c) LASER PROCESSED NiCrAlY



ADHERENT OXIDE SCALE
POROUS WHISKERS ON
ADHERENT OXIDES

OXIDE STRUCTURE OVER β NiCrAlY
TWO LAYER OXIDE STRUCTURE OVER BETA PHASE



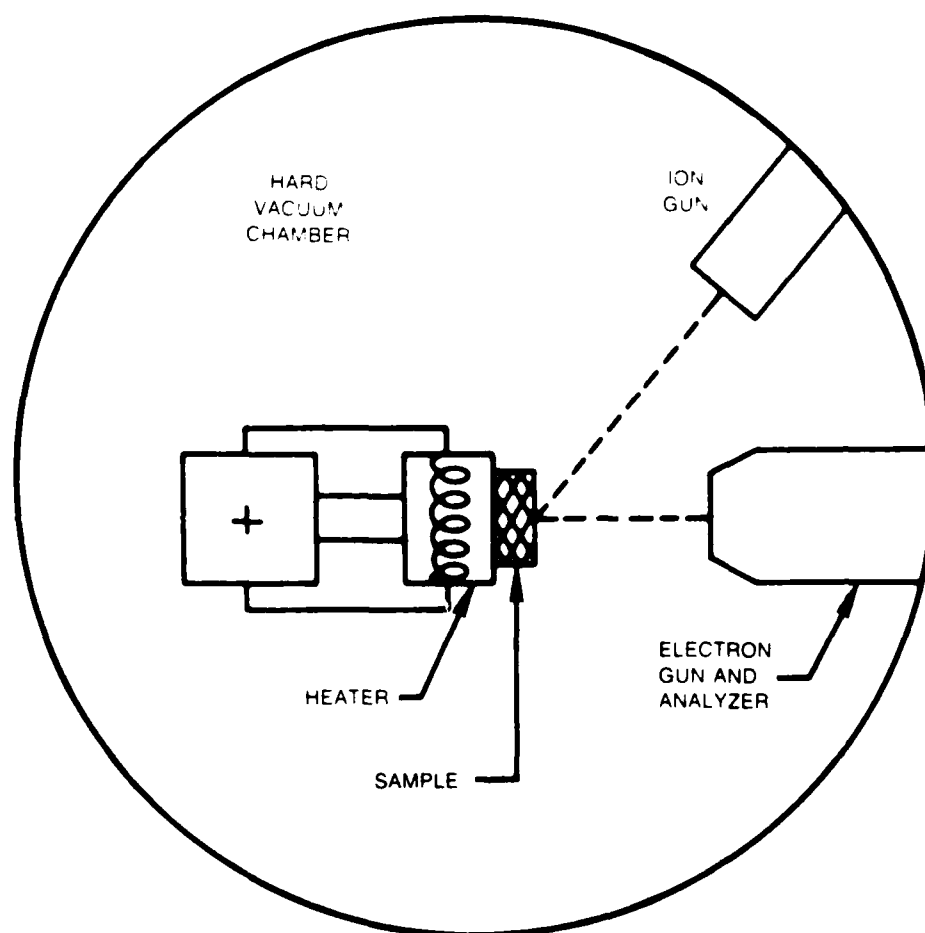
FIG. 4

FIG. 5

CROSS SECTION OF ADHERENT SCALE ON LASER PROCESSED NiCrAlY



AUGER SPECTROMETER AND SAMPLE HEATER



AUGER SPECTROSCOPY STUDIES

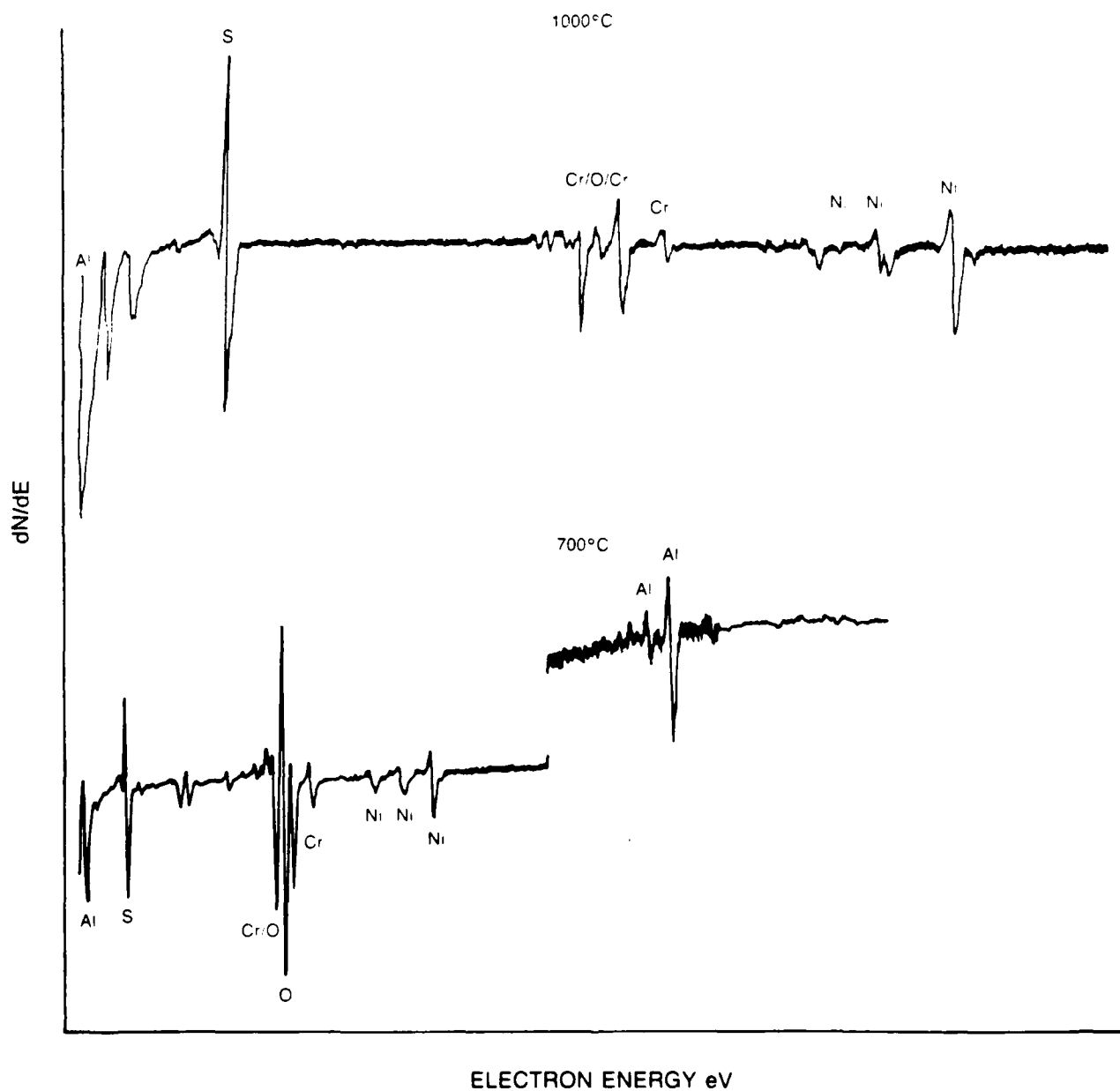
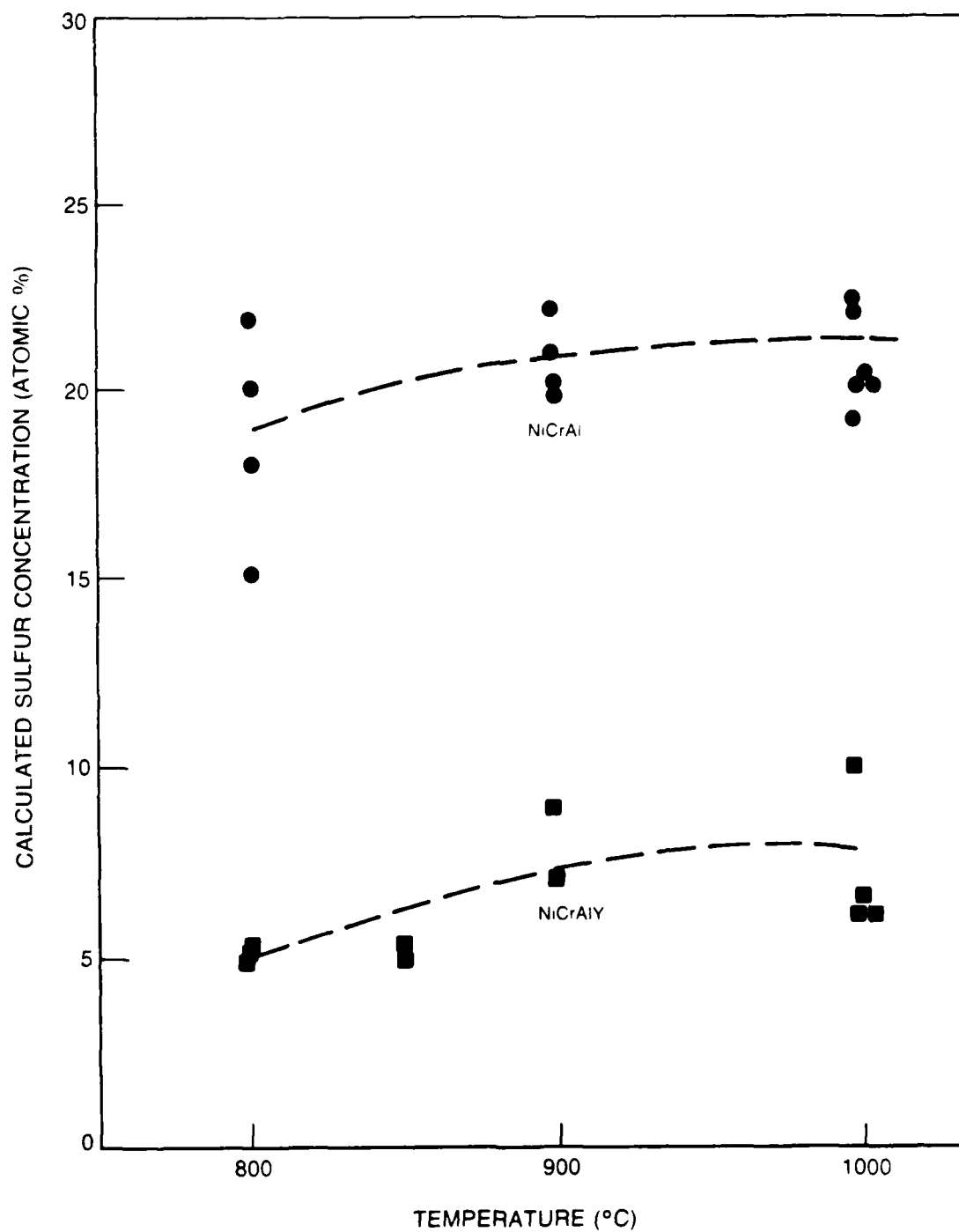


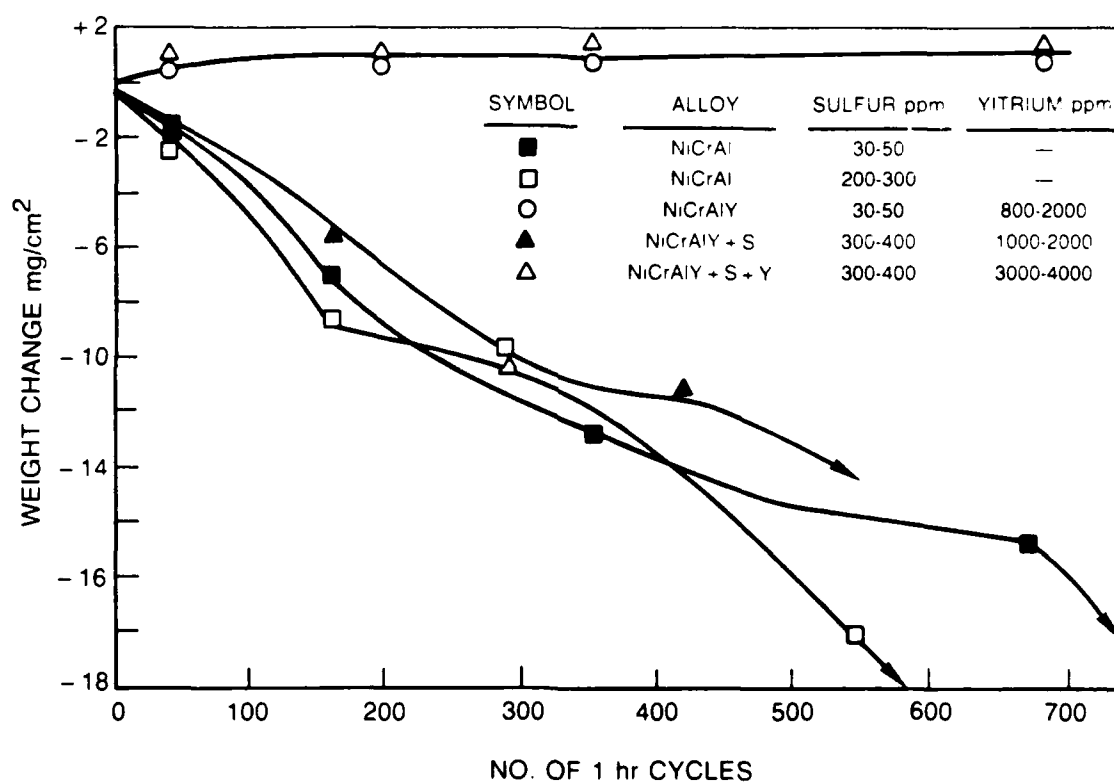
FIG. 8

SURFACE CONCENTRATION OF SULFUR VS TEMPERATURE



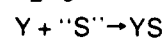
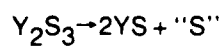
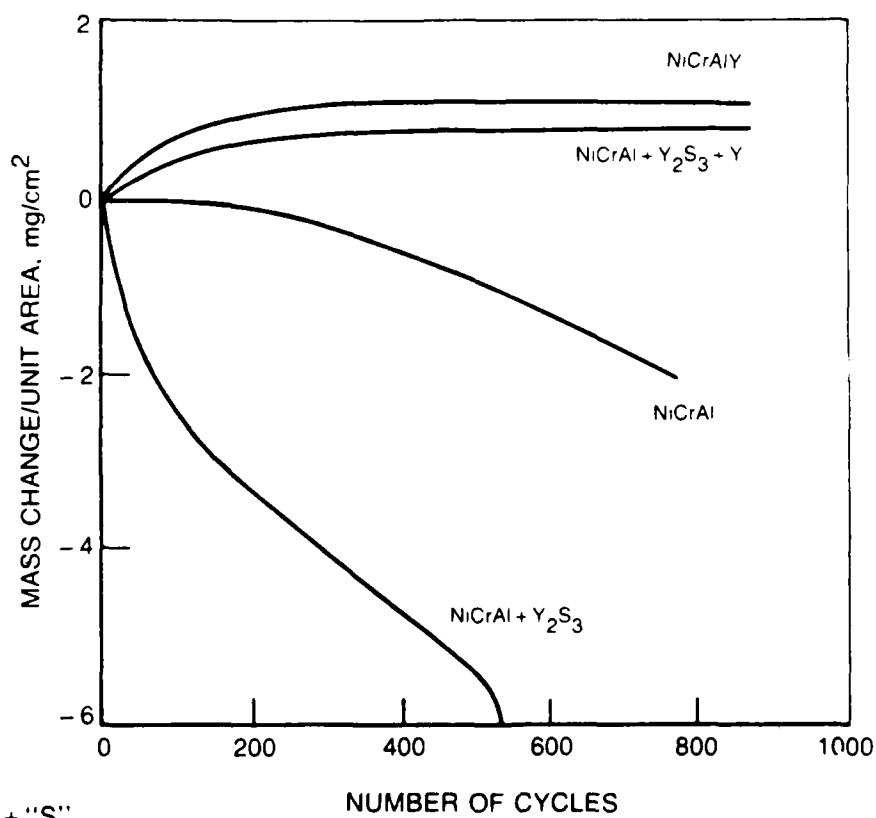
CYCLIC OXIDATION OF NiCrAl (Y) AT 1150°C

(1 hr CYCLES)

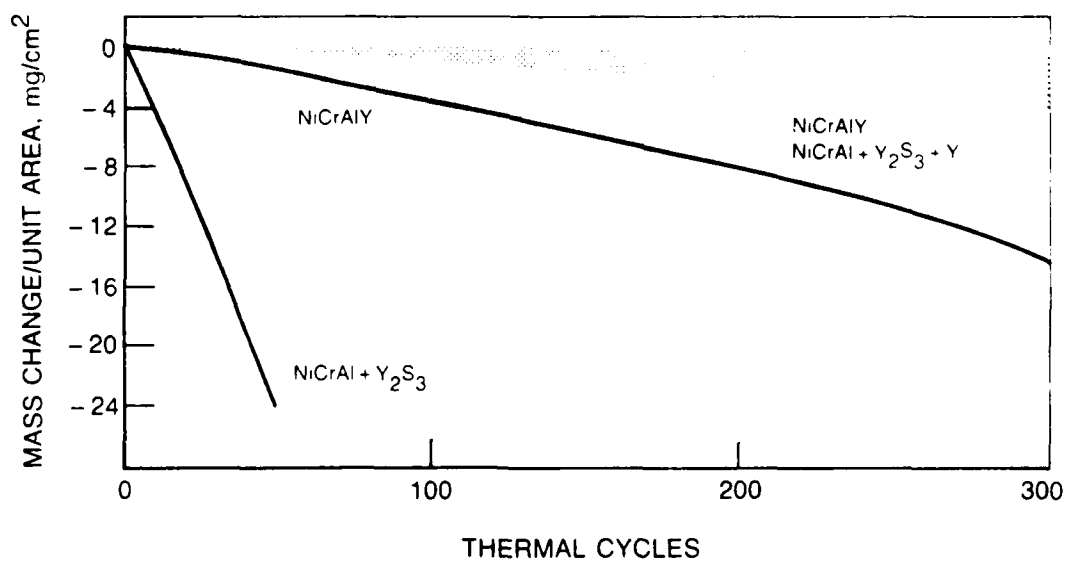


SULFUR INCREASES OXIDATION RATES

(1050°C)

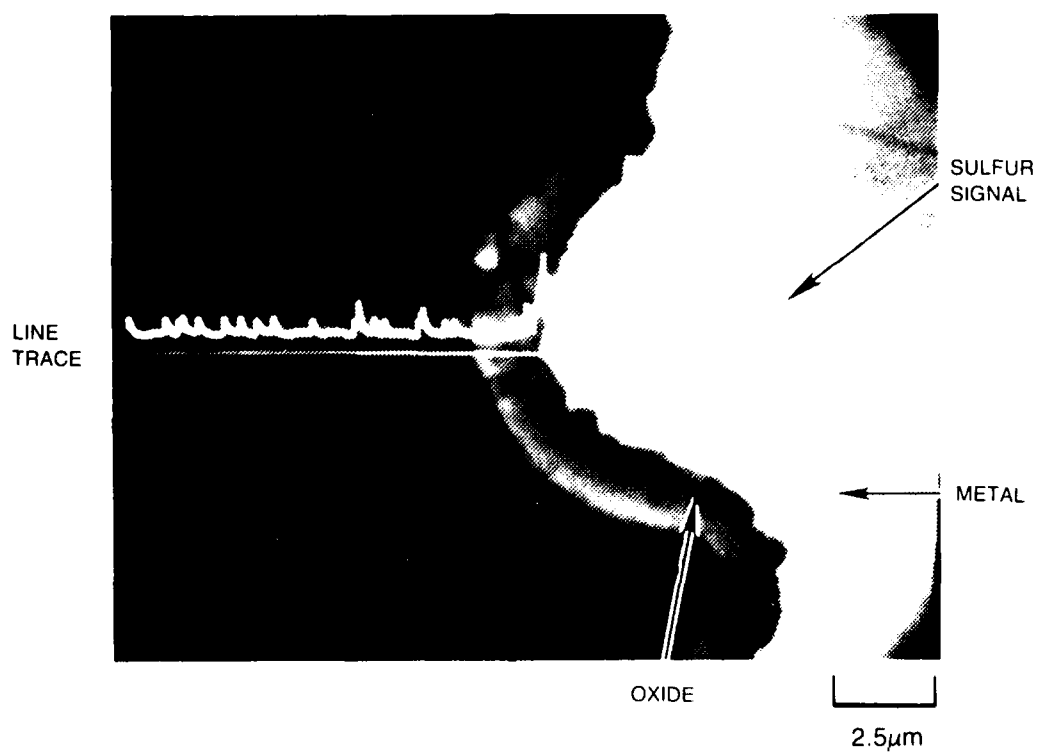


1180°C CYCLIC OXIDATION RESULTS



SULFUR SEGREGATION TO OXIDE/METAL INTERFACE

SULFUR X-RAY LINE TRACE



BINDING ENERGY FOR VARIOUS SULFUR-CONTAINING COMPOUNDS

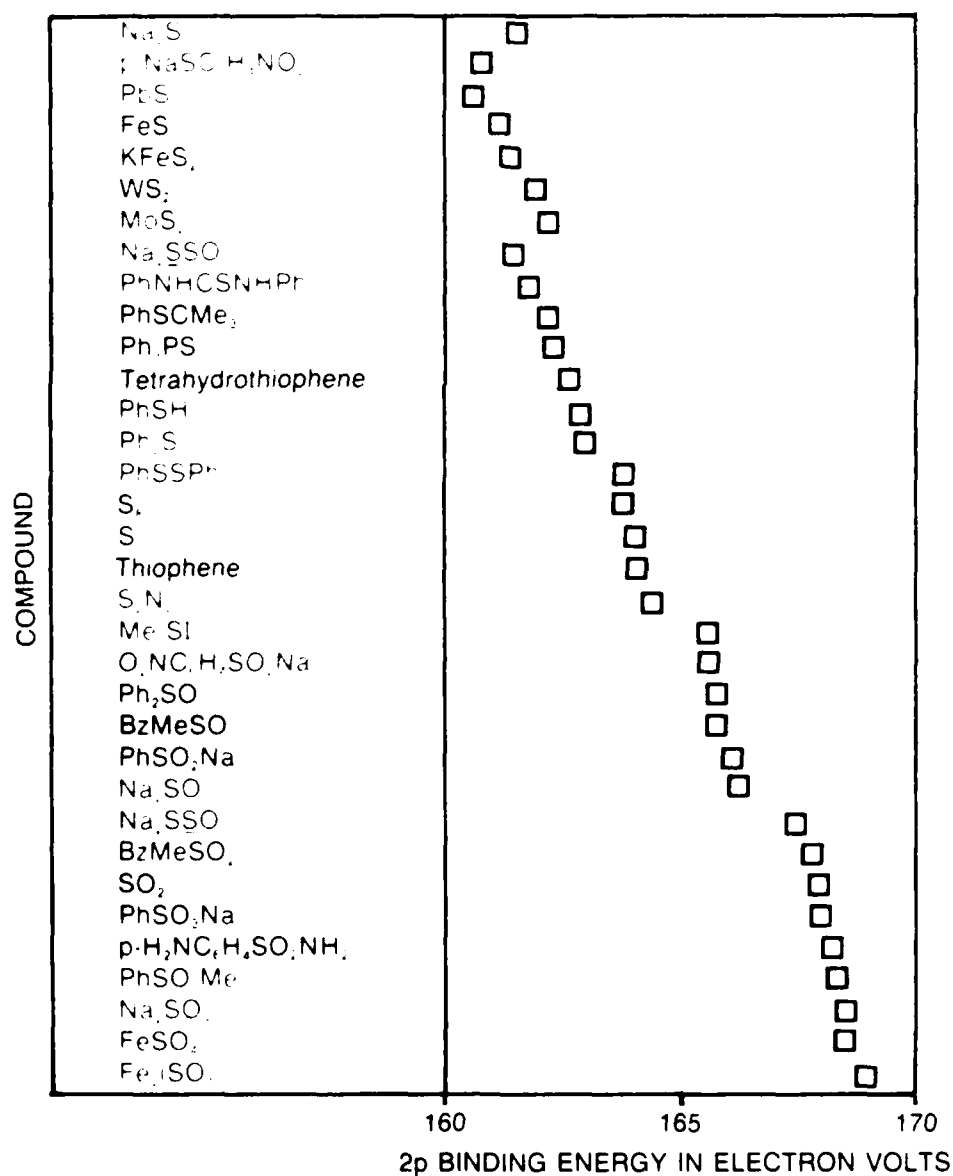
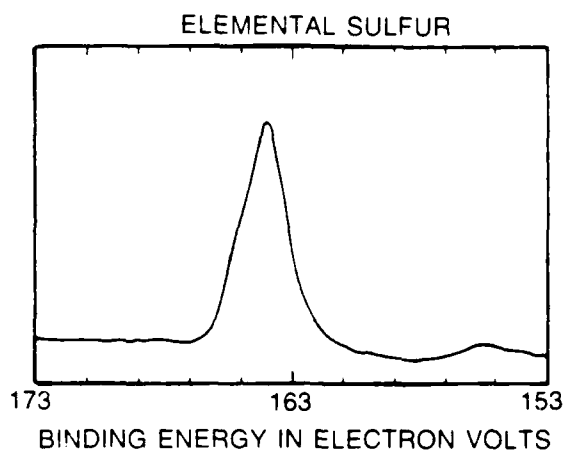


FIG. 14

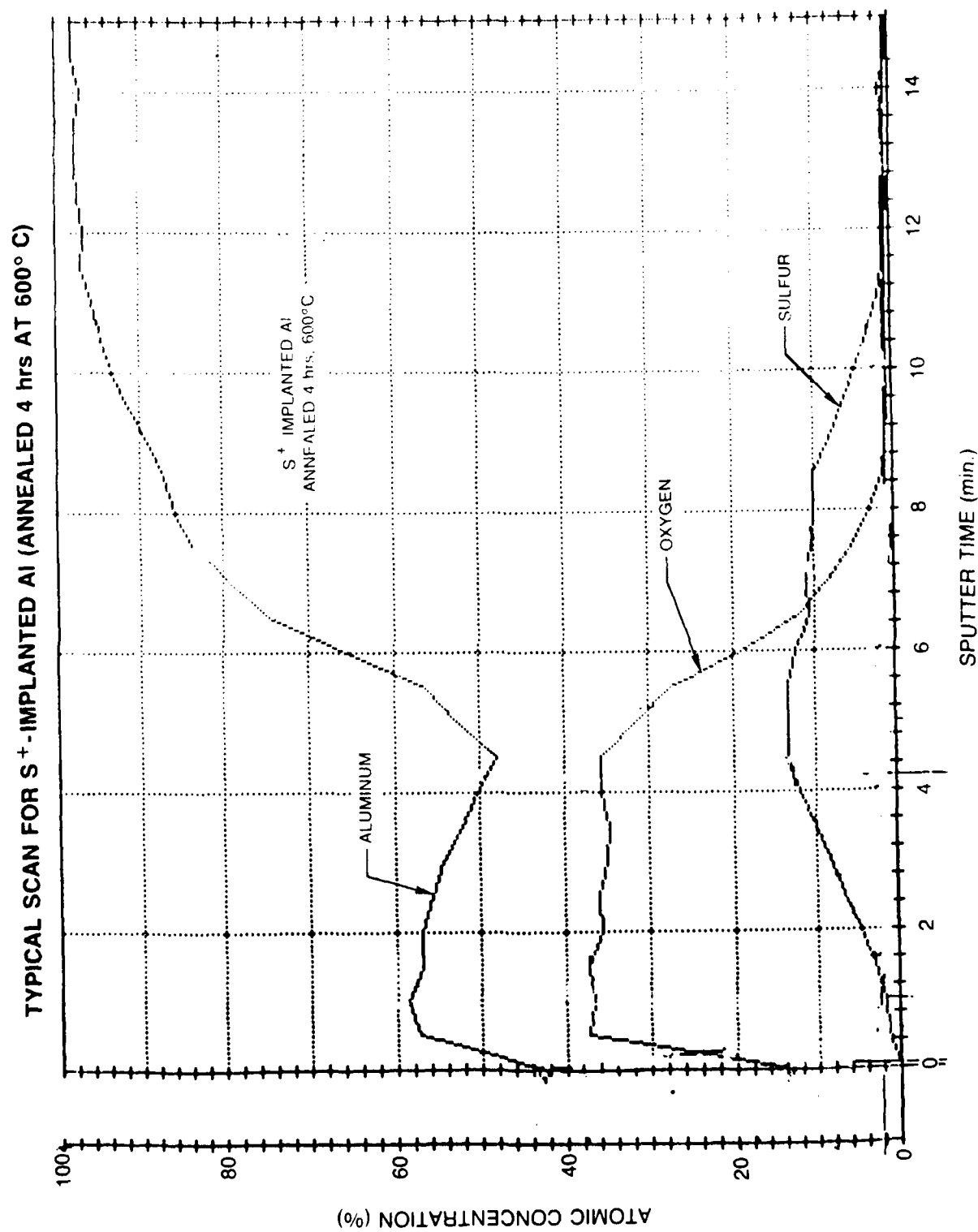
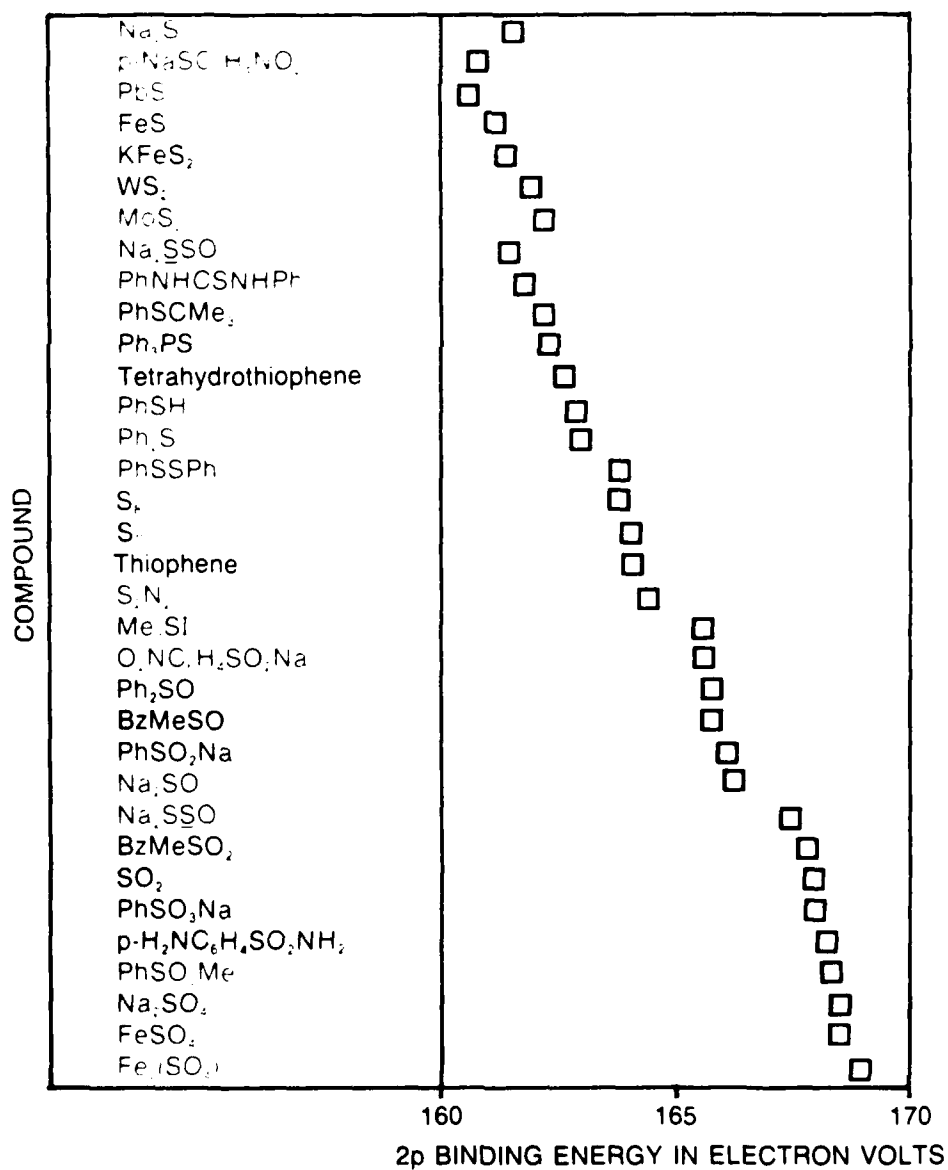
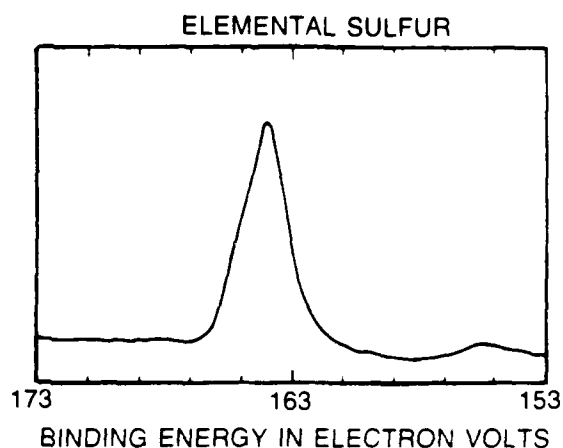


FIG. 15

BINDING ENERGY FOR VARIOUS SULFUR-CONTAINING COMPOUNDS

EXPERIMENTALLY
DETERMINED
BINDING ENERGY
FOR METAL SULFIDES

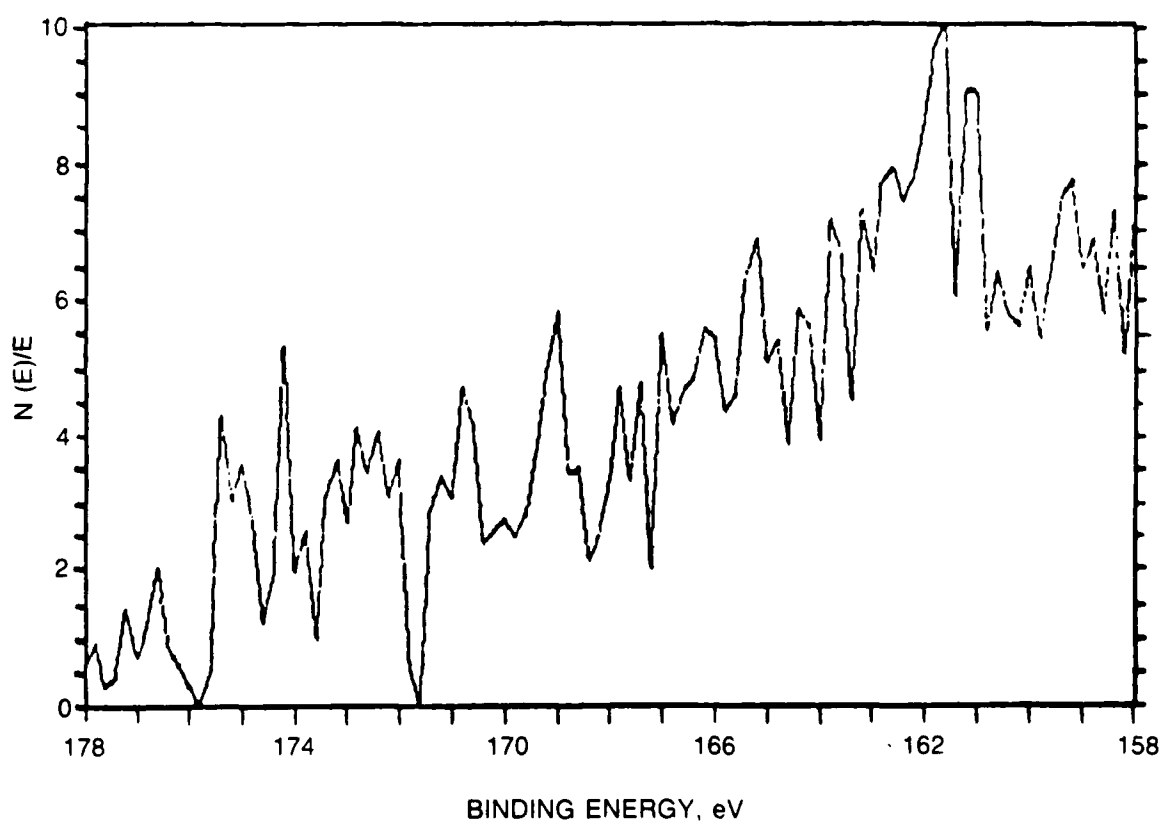
| | eV |
|--------------------------------|--------|
| Al | 161.91 |
| Al (ANNEALED) | 161.8 |
| Cr | 161.94 |
| Ni | 161.93 |
| Ni (ANNEALED) | 162.0 |
| Al ₂ O ₃ | 162.0 |



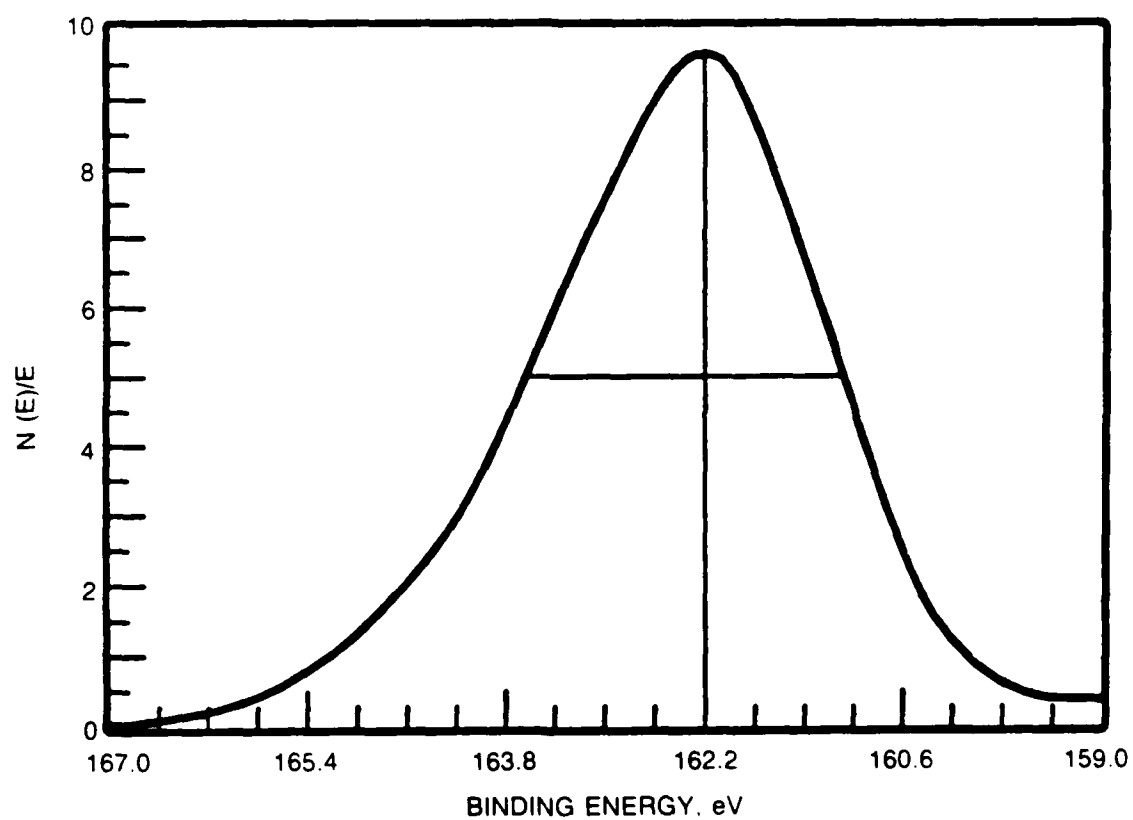
ESCA STUDIES

SHORT TIME DATA

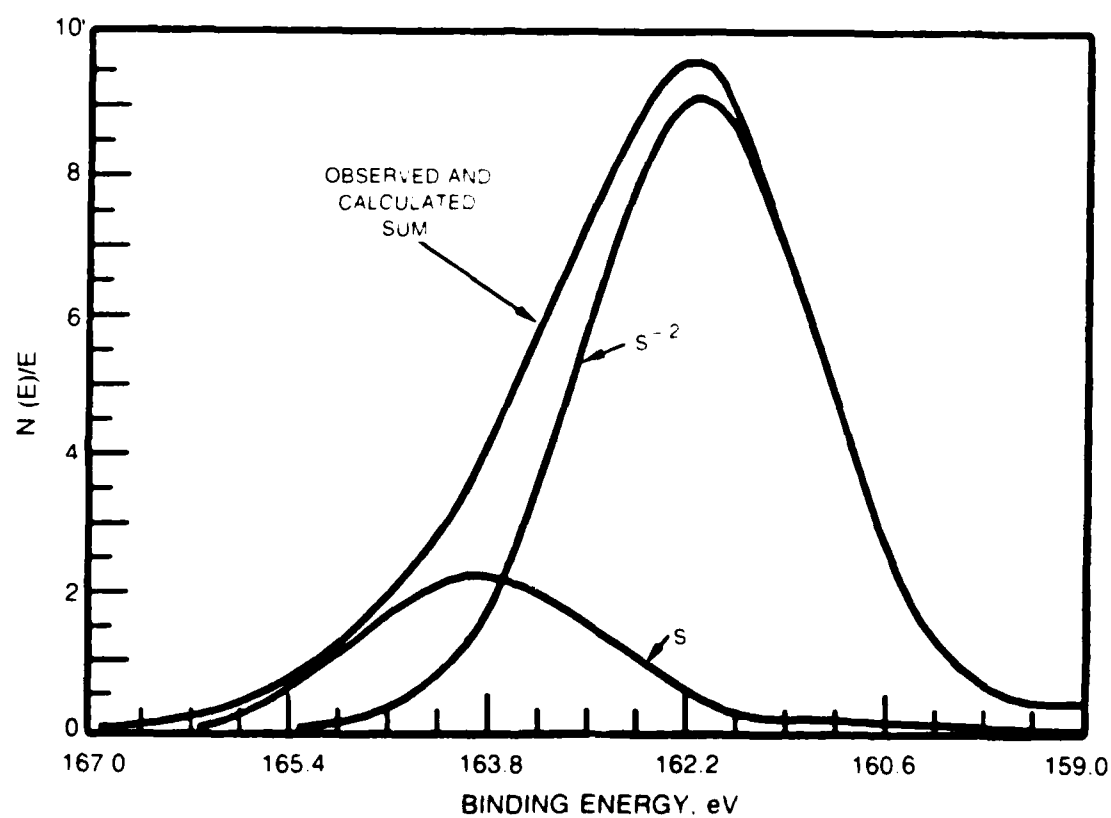
(2 min)



ESCA STUDIES
LONG TIME DATA COLLECTION: 19 HOURS
ASYMMETRIC PEAK



ESCA STUDIES
LONG TERM DATA COLLECTION (9 HOURS)



REFERENCES

1. Whittle, D.P. and J. Stringer, Philos. Trans. R. Soc. London Ser Vol A295, pp. 309-329 (1980).
2. Tien, J.K. and F.S. Petit: Met Trans Vol. 3, pp. 1587-1599 (1972).
3. Antill, J.E. and K.A. Peakall: J. Iron Steel Inst. Vol. 205, pp. 1136-1142 (1967).
4. Golightly, F.A., F.H. Stott and G.C. Wood: Oxid Met Vol. 10, pp. 163-187 (1976).
5. Pfeiffer, H: Werkst Korros Vol. 8, pp. 574-579, (1957)
6. McDonald, J.E. and J.G. Eberhart; Met Trans Vol. 233, pp.512-517 (1965).
7. Handbook of Auger Electron Spectroscopy, 2nd Ed. by L.E. Davis, N.C. McDonald, P.W. Palmberg, G.E. Riach and R.E. Weber, pp. 5-18 published by Perkin-Elmer Corp., Eden Prairie, Minn 1959.
8. Smeggil, J.G., A. W. Funkenbush and N.S. Bornstein; Thin Solid Films, Vol. 119, pp. 327-335 (1984).
9. Smeggil, J.G., A. W. Funkenbusch and N.S. Bornstein; A Study of Adherent Oxide Formation, Annual Report R83-916154-1, Office of Naval Research, Contract N00014-82-0618, Oct. 1983.
10. Smeggil, J.G., A. W. Funkenbusch and N.S. Bornstein; Met. Trans. Vol. 17A, pp. 923-930 (June 1986).
11. Doser M. and J.G. Smeggil; IEEE Trans Mag. Vol. May 9, pp. 168-171 (1973).
12. C.L. White, J. H. Schneibel and R. A. Podgett; Metall. Trans. A. 1983 Vol. 14A, p. 595.
13. H. Chaung, J.B. Lumsden and R.W. Stachle; Metall. Trans. 1974, Vol. 10, p. 1853.
14. R. A. Mulford, Metall. Trans A 1983, Vol. 14A, pg. 865.
15. J.E. Doherty, A.F. Giamei and B.H. Kear; Can Met Quart 1974, Vol. 13, p. 229.
16. M.P. eSah and C. Lea; Phil Mag 1975, Vol. 31, p. 627.
17. K. Yoshihara, M. Kurahushi and K. Nii, Trans Japan Inst. Met 1980, Vol. 21, p. 425.
18. L.A. Harris, Journal of Applied Physics 1968, Vol. 39, p.1428.
19. E. Sickatus, Surface Science 1970 Vol. 19, pg. 181.

20. P.H. Holloway and J.R. Hudson; Surface Science, 1972 Vol. 33 pg. 56.
21. H. Chaung, J.B. Lumsden and R.W. Stachle; Metall. Trans. 1974 Vol. 10, pg. 1853.
22. S. Mroz, C. Kosiol and J. Kolaczkievics; Vacuum 1975, Vol. 26, p. 61.
23. J.J. Burton, B.J. Berkowitz and R.D. Kane; Metall. Trans A, 1979 Vol. 10A, p. 677.
24. Wagner, C.D., W.M. Riggs, L.E. Davis, J.F. Moulder, G.E. Mullenberg: Handbook of X-Ray Electron Spectroscopy, published by Perkin-Elmer Corp, Eden Prairie, Minn 1979.
25. Smeggil, J.G. and N.S. Bornstein; Study of Adherent Oxide Scales, Contract N00014-85-C-0421 Report R86-917259-1, Jan. 1987.
26. Oforka, N.C. and B.B. Argent; Journal of the Less Common Met, 1985 Vol. 114, p.97-109.
27. (a) Hagar, J.P. and J. F. Elliott; Met Trans 1967, Vol. 239, p. 513.
(b) Elliott, J.F. and M. Gleiser; Thermochemistry for Steel Making Vol. 1, pub. by Addison-Wesley Publishing Company.
28. Gschneidner, K.A. and N. Kippenhan; Thermochemistry of the Rare Earth Carbides, Nitrides and Sulfides for Steel Making, Rare Earth Information Center Report No. 15-RIC-5, Institute for Atomic Research, Iowa State University Ames, 1972.

ONR BASIC DISTRIBUTION LIST

| <u>Organization</u> | <u>Copies</u> | <u>Organization</u> | <u>Copies</u> |
|--|---------------|--|------------------|
| Defense Documentation Center Cameron Station Alexandria, VA 22314 | 12 | Naval Air Propulsion Test Center Trenton, NJ 08628 ATTN: Library | 1 |
| Office of Naval Research Department of the Navy 800 N. Quincy Street Arlington, VA 22217 ATTN: Code 431 | 3 | Naval Construction Battalion Civil Engineering Laboratory Port Hueneme, CA 93043 ATTN: Materials Division | 1 |
| Naval Research Laboratory Washington, DC 20375 ATTN: Codes 6000 6300 2627 | 1 1 1 | Naval Electronics Laboratory San Diego, CA 92152 ATTN: Electronic Materials Sciences Division | 1 |
| Naval Air Development Center Code 606 Warminster, PA 18974 ATTN: Dr. J. Deluccia | 1 | Naval Missile Center Materials Consultant Code 3312-1 Point Mugu, CA 92041 | 1 |
| Commanding Officer Naval Surface Weapons Center White Oak Laboratory Silver Spring, MD 20910 ATTN: Library | 1 | Commander David W. Taylor Naval Ship Research and Development Center Bethesda, MD 20084 ATTN: Code 012.5 | 1 1 |
| Naval Oceans Systems Center San Diego, CA 92132 ATTN: Library | 1 | Naval Underwater System Center Newport, RI 02840 ATTN: Library | 1 |
| Naval Postgraduate School Monterey, CA 93940 ATTN: Mechanical Engineering Department | 1 | Naval Weapons Center China Lake, CA 93555 ATTN: Library | 1 |
| Naval Air Systems Command Washington, DC 20360 ATTN: Code 310A Code 5304B | 1 1 | NASA Lewis Research Center 21000 Brookpark Rd. Cleveland, OH 44135 ATTN: Library | 1 |
| Naval Sea System Command Washington, DC 20362 ATTN: Code 05R | 1 | National Bureau of Standards Washington, DC 20234 ATTN: Metals Science and Standards Standards Division Ceramics Glass and Solid State Science Division Fracture and Deformation Division | 1 1 1 1 |

ONR DISTRIBUTION LIST

| <u>Organization</u> | <u>Copies</u> | <u>Organization</u> | <u>Copies</u> |
|---|---------------|--|---------------|
| Naval Facilities Engineering Command Alexandria, VA 22331 ATTN: Code 03 | 1 | Defense Metals and Ceramics Information Center Battelle Memorial Institute 505 King Avenue Columbus, OH 43201 | 1 |
| Scientific Advisor Commandant of the Marine Corps Washington, DC 20380 ATTN: Code AX | 1 | Metals and Ceramics Division Oak Ridge National Laboratory P.O. Box X Oak Ridge, TN 37380 | 1 |
| Army Research Office P.O. Box 12211 Triangle Park, NC27709 ATTN: Metallurgy & Ceramics Program | 1 | Los Alamos Scientific Laboratory P.O. Box 1663 Los Alamos, NM 87544 ATTN: Report Librarian | 1 |
| Army Materials and Mechanics Research Center Watertown, MA 02172 ATTN: Research Programs Office | 1 | Argonne National Laboratory Metallurgy Division P.O. Box 229 Lemont, IL 60439 | 1 |
| Air Force Office of Scientific Research/NE Building 410 Bolling Air Force Base Washington, DC 20332 ATTN: Electronics & Materials Science Directorate | 1 | Brookhaven National Laboratory Technical Information Division Upton, Long Island NY 11973 ATTN: Research Library | 1 |
| NASA Headquarters Washington, DC 20546 ATTN: Code RRM | 1 | Library Building 50, Room 134 Lawrence Radiation Laboratory Berkeley, CA | 1 |